

Characterizing the Downlink Transmission Power for WCDMA Networks in Multiservice Environments

Chie Dou and Liang-Luen Huang
Department of Electrical Engineering
National Yunlin University of Science and Technology
No. 123, Section 3, University Road
640 Touliu, Yunlin, TAIWAN

Abstract: - This paper characterizes the downlink transmission power for WCDMA networks in multiservice environments for both urban and suburban macro cells. To calculate the required transmission power for the user in the cell, various modeling approaches are used to investigate the orthogonality, the path loss, and the inter-cell interference ratio of the user. The variation and scattering pattern of the required transmission power for each service connection are observed as a function of distance between the base station (BS) and the mobile station (MS). The phenomena and their explanations presented in the paper concerning the WCDMA downlink power issues are important for the power control and admission control of the system.

Key-Words: - WCDMA, Downlink, Transmission power, Multiservice, Macro cell, Orthogonality

1 Introduction

As it is known that the WCDMA downlink transmission power is interference dependent. The interference can be either due to own cell or adjacent cells. WCDMA employs orthogonal codes in the downlink to separate users, and without any multipath propagation the orthogonality remains when the base station (BS) signal is received by the mobile. However, if there is sufficient delay spread in the radio channel, the mobile will see part of the BS signal as intra-cell multiple access interference. The orthogonality of one corresponds to perfectly orthogonal users. The impact of downlink orthogonality factor (OF) on WCDMA system performance has been deeply investigated in the literature recently [1]-[4]. By utilizing the relationship between the OF and the channel dispersion, it has been shown that the time-averaged OF can be determined from the channel delay profile [1]. In the downlink, different mobiles also experience different inter-cell interference from adjacent cells depending on the location. The other-to-own-cell interference ratio can be defined as the summation of the ratio of every other cell to own cell base station transmission power received by the user. The received power from a cell depends on the path loss from the transmitting BS to the mobile station (MS). Two commonly adopted propagation models for macro cell scenarios are Okumura-Hata model [5] and COST 231 Walfisch-Ikegami model [6]. Both models can be applied to urban and suburban areas with some modifications of

parameter setting. Since both the orthogonality factor and the inter-cell interference are location dependent, that is, their values are varied according to the distance between the BS and the MS, the received power by a user moving in the cell are affected by them as well as by the path loss.

This paper characterizes the downlink transmission power for WCDMA networks in multiservice environments for both urban and suburban macro cells. In Section 2, the equation of the required transmission power for each service connection to meet the target E_b/N_0 is first derived. To calculate the required transmission power for the MS, various modeling approaches are needed to model the orthogonality, the path loss, and the inter-cell interference ratio of the MS. In Section 3, the required transmission power for a MS moving away from the BS to the cell edge is calculated as a function of distance between the BS and the MS. Such calculations are performed 100 times and the results are plotted together to observe the power variations and scattering as a function of distance. Here, the term 'power scattering' signifies the deviation between 100 different samples of the calculated transmission power at the same distance. The standard deviation of the power scattering at each distance is computed. The power variations and power scattering observed in Section 3 for each service connection pertaining to different traffic classes are important for the system design, such as power control and admission control. Finally, in Section 4 the discussions and conclusions are given.

Table 1 Parameters and Definitions

Parameter	Definition
W	The chip rate
$N_j^{(m)}$	The number of users of class j in cell m
$\nu_{ij}^{(m)}$	The activity factor of user i of class j in cell m
$R_{ij}^{(m)}$	The bit rate of user i of class j in cell m
$P_{ij}^{(m)}$	The required transmit power for user i of class j from cell m
N_{rf}	The noise spectral density of the mobile receiver front-end
$P_{total}^{(m)}$	The total downlink transmission power of cell m
$L_{ij}^{(m)}$	The path loss from the serving cell m to user i of class j
$L_{ijm}^{(n)}$	The path loss from another cell n to user i of class j in cell m
$\alpha_{ij}^{(m)}$	The orthogonality factor of user i of class j in cell m
M	The number of cells in the system

2 Power Modeling Approaches

The required $(E_b/N_0)^m$ for user i ($i=1, \dots, N_j^{(m)}$) of class j ($j=1, \dots, K$) in cell m ($m=1, \dots, M$) is based on the link quality equation for the WCDMA downlink connection [7]:

$$\left(\frac{E_b}{N_0}\right)_{ij}^{(m)} = \frac{W}{\nu_{ij}^{(m)} \cdot R_{ij}^{(m)}} \cdot \frac{P_{ij}^{(m)} / L_{ij}^{(m)}}{(1 - \alpha_{ij}^{(m)}) \cdot P_{total}^{(m)} / L_{ij}^{(m)} + N_{rf} \cdot W + \sum_{n=1, n \neq m}^M P_{total}^{(n)} / L_{ijm}^{(n)}}. \quad (1)$$

The parameters used in (1) are explained in Table 1. Solving for $P_{ij}^{(m)}$ gives:

$$P_{ij}^{(m)} = \frac{(E_b/N_0)_{ij}^{(m)} \cdot \nu_{ij}^{(m)}}{W / R_{ij}^{(m)}} \left[(1 - \alpha_{ij}^{(m)}) \cdot P_{total}^{(m)} + \sum_{n=1, n \neq m}^M P_{total}^{(n)} \cdot \frac{L_{ij}^{(m)}}{L_{ijm}^{(n)}} + N_{rf} \cdot W \cdot L_{ij}^{(m)} \right]. \quad (2)$$

Assume that the total transmit power of different cells are equal. This assumption is approximately valid if there is a regular grid of base stations, and the traffic distribution is uniform. The total downlink transmission power of cell m can be written as

$$P_{total}^{(m)} = \sum_{j=1}^K \sum_{i=1}^{N_j^{(m)}} P_{ij}^{(m)} = \frac{N_{rf} \cdot W \cdot \sum_{j=1}^K \sum_{i=1}^{N_j^{(m)}} c_{ij}^{(m)} \cdot L_{ij}^{(m)}}{1 - \eta_{DL}}, \quad (3)$$

$$\text{where } c_{ij}^{(m)} = \frac{(E_b/N_0)_{ij}^{(m)} \cdot \nu_{ij}^{(m)}}{W / R_{ij}^{(m)}}, \quad (4)$$

$$\text{and } \eta_{DL} = \sum_{j=1}^K \sum_{i=1}^{N_j^{(m)}} [c_{ij}^{(m)} \cdot (1 - \alpha_{ij}^{(m)} + I_{ij}^{(m)})]. \quad (5)$$

In (5), $I_{ij}^{(m)} = \sum_{n=1, n \neq m}^M (L_{ij}^{(m)} / L_{ijm}^{(n)})$ is defined as the other-to-own-cell interference ratio received at user i of class j in cell m . In the downlink, this ratio depends on the user location and is therefore different for each user. To calculate the required transmit power for each

service connection using the equation expressed by (2), the three service-independent parameters $\alpha_{ij}^{(m)}$, $I_{ij}^{(m)}$, and $L_{ij}^{(m)}$, must be modelled properly first. The modelling approaches for these parameters adopted in this paper are described as follows.

2.1 Modeling the Orthogonality Factor

Assume that the impulse response of the macro cell radio channel can be modeled in discrete form as

$$h(\tau) = \sum_{l=0}^{L-1} \beta_l \delta(\tau - lT_c), \quad (6)$$

where $T_c = 1/W$ is the chip time, β_l is the complex amplitude of the l -th multipath component, and L denotes the total number of fingers. From (6), the average power delay profile (PDP) of the channel can be expressed as

$$P(\tau) = \sum_{l=0}^{L-1} E[|\beta_l|^2] \delta(\tau - lT_c), \quad (7)$$

where $E[\cdot]$ denotes spatial averaging over the fast fading. We will assume Rayleigh fading characteristics, i.e., $E[|\beta_l|^2] = |\beta_l|^2$, and an exponential decaying PDP $|\beta_l|^2$ according to COST 259 [8]

$$|\beta_l|^2 = \frac{e^{-lT_c/\tau_{rms}}}{\sum_{l'=0}^{L-1} e^{-l'T_c/\tau_{rms}}}, \quad (8)$$

where τ_{rms} is the RMS delay spread (DS). The Greenstein model [9] suggests that τ_{rms} is lognormal at every base-to-mobile distance d , with a median that grows mildly with d and a decibel standard deviation that is independent of d . The DS at distance d between the BS and the MS can therefore be expressed as

$$\tau_{rms} = T_1 d^\varepsilon y, \quad (9)$$

where T_1 is the medium value of τ_{rms} at distance $d=1$ Km, ε is an exponent that lies between 0.5-1.0, and y is a lognormal variate. Specifically, $Y = 10 \log y$ is a Gaussian random variable over the terrain at distance d , having zero mean and a standard deviation, σ_y , that lies between 2-6 dB.

An approximate formula for the OF is presented in [1] for the case where the total received wideband power is much greater than the inter-cell interference and the noise power,

$$\alpha = 1 - \left[\sum_{m=1}^M \frac{|\beta_m|^2}{\sum_{l=1, l \neq m}^L |\beta_l|^2} \right]^{-1}, \quad (10)$$

where M is the number of Rake fingers. The value of M is selected so that all resolvable multipath components can capture certain percentage of total power. Clearly, at each d the larger M implies the greater OF. In this study we assume $L=6$ and the

value of M is selected so that 95% total power is captured. In general, the OF is decreased as d increases; however, violations may be occurred due to the change in the number of active Rake fingers.

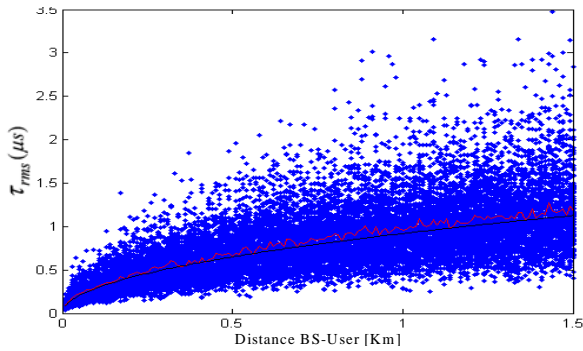


Fig. 1 The τ_{rms} versus d for the urban cell.

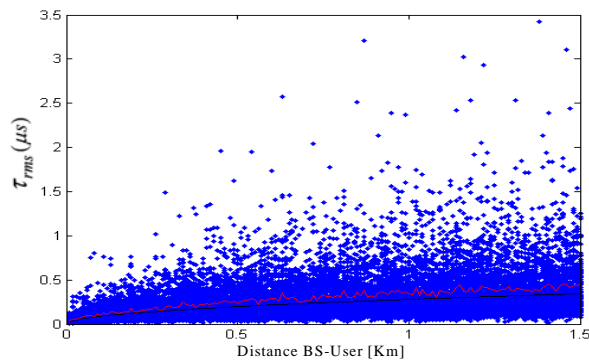


Fig. 2 The τ_{rms} versus d for the suburban cell.

To calculate the RMS DS and the OF for a MS in the cell with cell radius 1.5 Km, we adopted the parameters suggested in [9] for the Greenstein model. Toronto urban area with $T_1=0.92$ us and $\sigma_y=1.9$ dB is assumed for the urban cell conditions. For suburban macro cell conditions, Toronto suburban area with $T_1=0.28$ us and $\sigma_y=4.7$ dB is assumed. For both urban and suburban areas $\epsilon=0.5$ is used. Fig. 1 and Fig. 2 show the τ_{rms} (in us) versus the distance d for the urban and suburban cell conditions, respectively. At each distance d we take 100 samples for the τ_{rms} . Clearly, the values of the sampled τ_{rms} scattered with respect to the median T_1d^ϵ . The curve for the T_1d^ϵ versus the distance d is drawn in the figures as a smooth curve. Also, the sampled mean at each d for the τ_{rms} is plotted along with the median curve. Clearly, the RMS DS for the urban cell is greater than that for the suburban cell.

Given the τ_{rms} calculated by (9), the associated OF for the user can be obtained from (8) and (10). Fig. 3 and Fig. 4 show the OF versus the distance d for the urban and suburban cell conditions, respectively. Corresponding to the 100 sampled τ_{rms} at each d calculated in Figs. 1 and 2, we also have

100 sampled OF at each d in Figs. 3 and 4. In Fig. 3 it can be observed that for the urban cell the OF decaying sharply as d is small (from 0 to 0.5 Km). As d becomes larger ($d > 0.5$ Km), the changing of the OF becomes slowly. In Fig. 4 we observe that the sampled mean of the OF at each d for the suburban cell decaying smoothly as d increases. Compare Fig. 3 and Fig. 4, we observe the following different characteristics of the OF for the urban and suburban macro cells. First, the scatter pattern of the OF for the urban cell shown in Fig. 3 becomes convergent as d becomes larger. However, the scatter pattern for the suburban cell shown in Fig. 4 is still divergent as d becomes larger. This important observation has great influence on the behaviors of different power variations for the users in the urban and suburban cells, as we will explain in the next section. Second, at the same d the OF for the suburban cell is larger than that for the urban cell. In general, the OF for the suburban areas is greater than 0.5, and the OF for the urban areas is smaller than 0.3 as $d > 0.5$ Km. From (2) it is clear that the larger OF implies the smaller required transmission power for the MS.

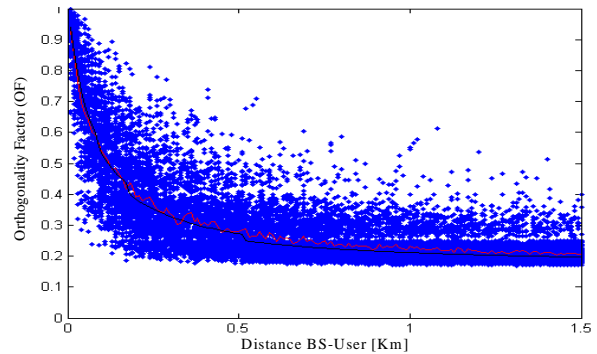


Fig. 3 The OF versus d for the urban cell.

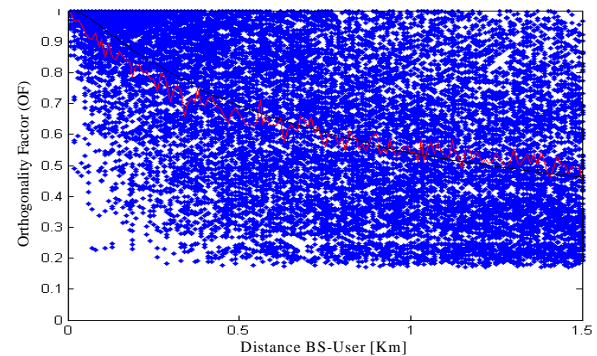


Fig. 4 The OF versus d for the suburban cell.

2.2 Modeling the Path Loss

Two commonly adopted propagation models for macro cell scenarios: Hata model and COST 231 WI model are used to calculate the path loss for the MS. The Hata model for an urban cell with base station

antenna height of 30 m, mobile antenna height of 1.5 m and carrier frequency of 1950 MHz is [5] $L = 137.4 + 35.2 \log_{10}(d)$, where L is the path loss in dB. The path loss for a suburban cell with an additional area correction of 8 dB is [5] $L = 129.4 + 35.2 \log_{10}(d)$. In the Hata model, the path loss is determined only by one parameter, d ; however, in the COST-WI model more complex situations are considered. Specifically, in the WI-model we assume the building separation for the urban cell is 20 m and for the suburban cell is 40 m; the widths of roads for the urban cell is 10 m and for the suburban cell is 20 m. For both urban and suburban cells we assume the heights of buildings is 15 m and the non-line-of-sight (NLOS) situations are considered. In addition, the road orientation with respect to the direct radio path φ is considered. Fig. 5 plots the path loss versus the distance d (varies from 0.75 Km to 1.5 Km) for both Hata and COST-WI models. The mobile moves horizontally with initially $\varphi = 90^\circ$ and $d=0.75$ Km. From Fig. 5 we observe that the path loss for the urban cell is larger than that for the suburban cell, and the path loss calculated by the COST-WI model is larger than that calculated by the Hata model.

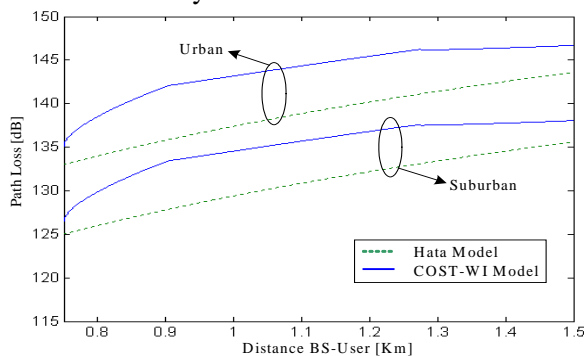


Fig. 5 The path loss of the MS versus d .

2.3 Modeling the Inter-Cell Interference

Fig. 6 plots the other-to-own-cell interference ratio versus the distance d , using the path loss obtained in Fig. 5. In this study we assume a symmetric 19 cells cellular model with an omnidirectional antenna covers each cell of hexagonal shape. From Fig. 6 we observe that the urban cell and the suburban cell have the same other-to-own-cell interference ratio. This is because the other-to-own-cell interference ratio is defined as the summation of individual ratios between the path losses from the serving cell and from another cell to the MS. Although the path loss calculations for urban and suburban situations are different, the division operation between path losses eliminates this difference. Thus, there have only two

curves shown in Fig. 6 but not four curves. In Fig. 6 we notice that the other-to-own-cell interference ratio calculated by the COST-WI model is larger than that calculated by the Hata model as $d < 1.5$ Km. The curve obtained by the Hata model increases exponentially, however the curve obtained by the COST-WI model can be divided into three parts due to three different conditions of street-orientation function. The first part of the curve corresponds for $55^\circ \leq \varphi < 90^\circ$ and increases sharply than that obtained by the Hata model. The second part of the curve corresponds for $35^\circ \leq \varphi < 55^\circ$, and the third part of the curve corresponds for $\varphi < 35^\circ$. From (2) it is clear that the larger other-to-own-cell interference ratio implies the larger required transmission power for the MS.

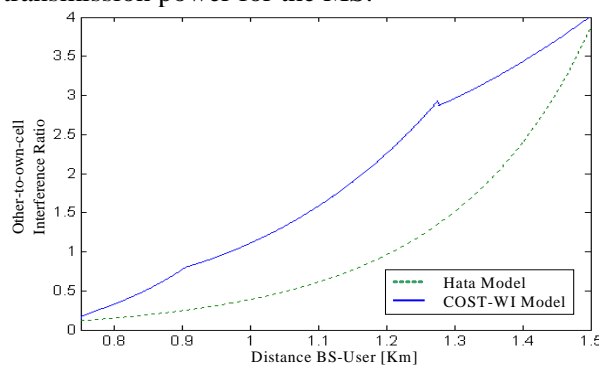


Fig. 6 The inter-cell interference ratio versus d .

3 Power Variations and Scattering

This study considers three QoS classes shared on a WCDMA downlink, including AMR speech, VoIP, and Video streaming. To compute the transmit power for each active user pertaining to different classes by (2), the following assumptions of parameters are used: $N_{rf}W = -103.16$ dBm/Hz; the channel symbol rate for AMR users is 20.13 Kbps, for VoIP users is 18.5 Kbps, for Video users is 36.8 Kbps; the target E_b/N_0 for AMR users is 5.5 dB, for VoIP users is 4.5 dB, for Video users is 6.5 dB; the activity factor for both AMR and VoIP is 0.67, for Video is one. Fig. 7 shows the required transmission power for a Video user moving from the BS toward the cell edge as a function of d . Obviously, the mobile in the urban cell required more transmission power than in the suburban cell. The power variation for the suburban cell is much greater than that in the urban cell. To simplify the presentation only the results obtained by the Hata propagation model are shown in here. To observe the power variation and scattering conditions for Video users in the cell as a function of distance, 100 different calculations same as that obtained in Fig. 7

are performed and their results are plotted together. Figs. 8(a) and 9(a) show the required transmission power versus the distance d obtained for the Video users in the urban cell and suburban cell, respectively. Since at each d one hundred samples are generated, the standard deviation of these samples represents the degree of power scattering at that distance. Figs. 8(b) and 9(b) show the standard deviation of the required transmission power versus the distance d obtained for the Video users in the urban and suburban cell, respectively. Clearly, the dotted area shown in Fig. 9(a) is much larger than that shown in Fig. 8(a). It is interested to notice that the standard deviation of the required transmission power for the user in the urban cell goes downwardly with fluctuation as d increases; however, the standard deviation of the required transmission power for the suburban cell almost keep steadfast as $d > 0.5$ Km. The main reason that causes this difference is due to the modeling of the orthogonality factor. In (2), the required transmission power for the user is determined by the three terms in the square bracket. The last two terms, one is related to the inter-cell interference ratio and the other is related to the path loss, have no scatter conditions at each distance d . Thus we know that the power scattering patterns as shown in Figs. 8(a) and 9(a) are caused by the $\alpha_{ij}^{(m)}$ in (2), that is the OF of the user. Since for the urban cell, as d increases the scatter pattern of the OF becomes convergent, that is the deviations of the sampled values for the OF become smaller. Hence, the standard deviation of the required transmission power for the Video users in the urban cell goes downwardly as shown in Fig. 8(b), from about 20 dBm to 14 dBm, as d increases. Contrarily, the scatter patten of the OF for the suburban cell remains divergent, that is the deviations of the sampled values for the OF almost hold the same distribution, as d increases. Hence, the standard deviation of the transmission power for the Video users in the suburban cell almost keep steadfast as shown in Fig. 9(b), between 22-23 dBm, as $d > 0.5$ Km.

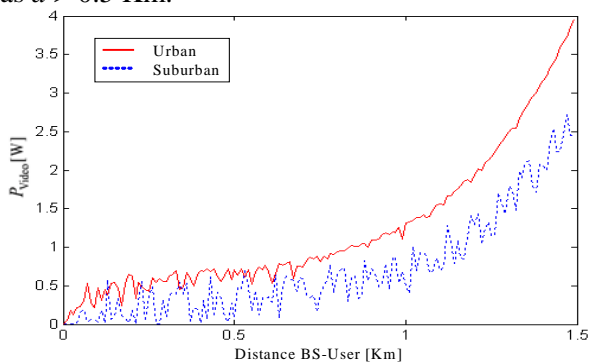


Fig. 7 The required transmit power for a Video user.

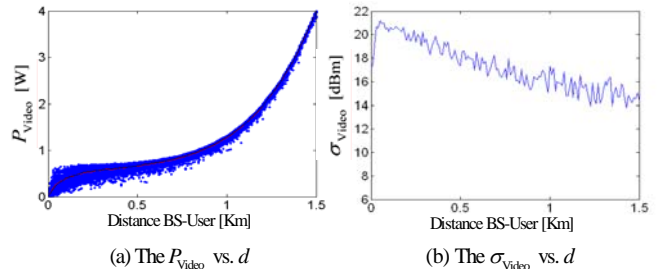


Fig. 8 The P_{Video} and σ_{Video} vs. d in urban cell.

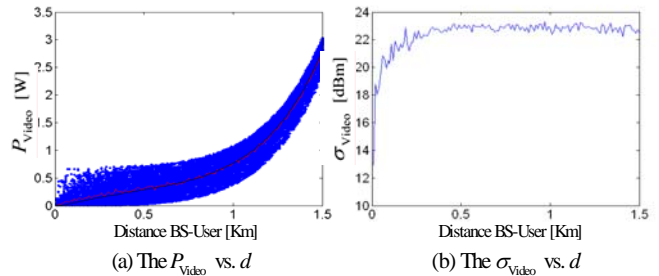


Fig. 9 The P_{Video} and σ_{Video} vs. d in suburban cell.

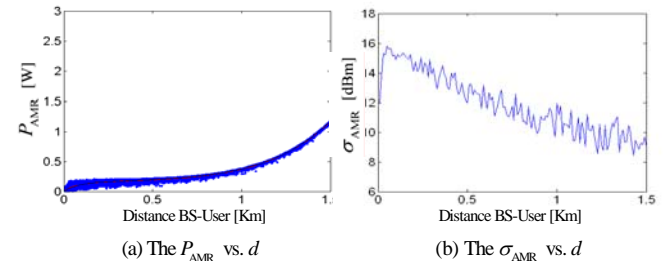


Fig. 10 The P_{AMR} and σ_{AMR} vs. d in urban cell.

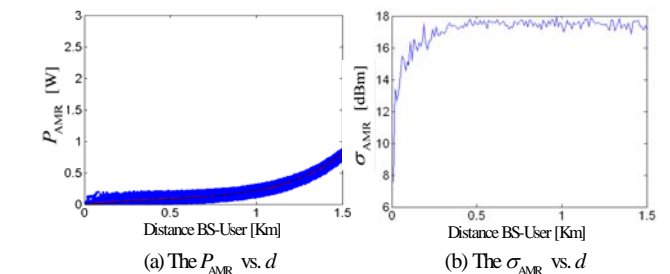


Fig. 11 The P_{AMR} and σ_{AMR} vs. d in suburban cell.

Figs. 10 and 11 show the required transmission power and its standard deviation for the AMR users in the urban and in the suburban cell, respectively. As the same Figs. 12 and 13 are plotted for VoIP users. The trends for the standard deviation of the required transmission power for the users of different service classes, as shown in Figs. 8(b), 10(b), and 12(b), are the same for the urban cell, that is, all goes downwardly as d increases. In Fig. 10(b), the standard deviation goes down from 15 dBm to 9 dBm, with a difference of 6 dBm. In Fig. 12(b), the standard deviation goes down from 14 dBm to 8 dBm, with a difference of 6 dBm also. Actually, this difference of 6 dBm has already appeared in Fig. 8(b). For the suburban cell, the trends shown in Figs. 9(b), 11(b), and 13(b) are also similar, that is, all keep steadfast as d increases. For

AMR users, the standard deviation keeps steadfast at about 17 dBm. For VoIP users, the standard deviation keeps steadfast at about 16 dBm. Compare the required transmission power and its standard deviation for the users of different service classes, we find that in both urban and suburban cell the order of their magnitudes is Video>AMR> VoIP.

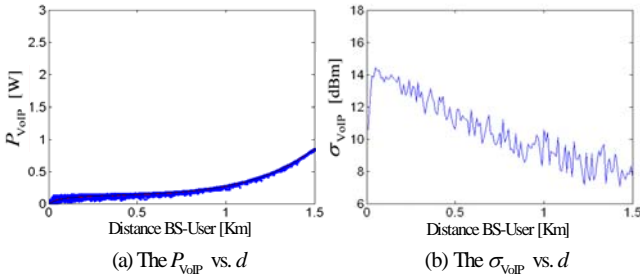


Fig. 12 The P_{VoIP} and σ_{VoIP} vs. d in urban cell.

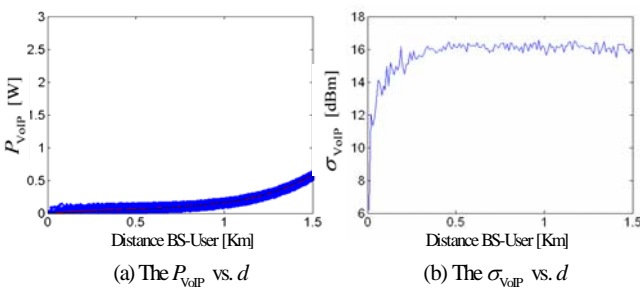


Fig. 13 The P_{VoIP} and σ_{VoIP} vs. d in suburban cell.

4 Conclusions

This paper characterizes the downlink transmission power for WCDMA networks in multiservice environments for both urban and suburban macro cells. To satisfy the QoS requirement of each service connection, the BS must provide the required transmission power for the MS continuously. To calculate the required transmission power for the MS, various modeling approaches are adopted to model the orthogonality, the path loss, and the inter-cell interference ratio of the MS. For a WCDMA downlink, the BS total transmission power is shared by all connections pertaining to different service classes. The understanding of the power characteristics for each individual connection as well as the aggregation of service connections is helpful in designing the power control and admission control algorithms of the system. A system with well-designed power control and admission control can not only lower the dropping and blocking probabilities of the calls but also increase the number of active calls in the cell, thus enhance the system capacity. However, these topics are beyond the scope of this study. In (2), the required transmission power for the user is determined by the three terms in the square bracket.

The last two terms, one is related to the inter-cell interference ratio and the other is related to the path loss, have no scatter conditions at each distance d . Thus we know that the power scattering patterns as shown in Figs. 8(a) and 9(a) are caused by the $\alpha_{ij}^{(m)}$ in (2), that is the OF of the user. This study observes many interesting phenomena concerning the WCDMA downlink power issues and their explanations are also provided. For instance, the standard deviation of the required transmission power for the user in the urban cell goes downwardly as d increases, however, for the suburban cell it almost keeps steadfast as $d > 0.5$ Km. The reason is that for the urban cell as d increases the scatter pattern of the OF becomes convergent, however, the scatter pattern of the OF for the suburban cell remains divergent, that is the deviations of the sampled values for the OF almost keep the same distribution, as d increases.

References:

- [1] N.B. Mehta, L.J. Greenstein, T.M. Willis, and Z.Kostic, Analysis and results for the orthogonality factor in WCDMA downlinks, in *Proc. IEEE VTC 2002-Spring*, pp. 100-104.
- [2] K.I. Pedersen and P.E. Mogensen, The downlink orthogonality factors influence on WCDMA system performance, in *Proc. IEEE VTC 2002-Fall*, pp. 2061-2065.
- [3] O. Awoniyi, N.B. Mehta, and L.J. Greenstein, Characterizing the orthogonality factor in WCDMA downlinks, *IEEE Trans. on Wireless Communications*, vol. 2, no. 4, July 2003.
- [4] C. Passerini and G. Falciasecca, Modeling of orthogonality factor using ray-tracing predictions, *IEEE Trans. on Wireless Communications*, vol. 3, no. 6, Nov. 2004.
- [5] H. Holma and A. Toskala, (Editors), *WCDMA for UMTS – Radio Access for Third Generation Mobile Communications*, revised ed., John Wiley & Sons, Chichester, England, 2001.
- [6] E. Damosso and L.M. Correia (Editors), *COST 231 - Digital mobile radio towards future generation systems*, Final Report, European Commission–COST Telecom Secretariat, Brussels, Belgium, 1999.
- [7] K. Sipilä, Z.C. Honkasalo, J.L. Steffens, and A. Wacker, Estimation of capacity and required transmission power of WCDMA downlink based on a downlink pole equation, in *Proc. IEEE VTC-Spring 2000*, pp. 1002-1005.
- [8] L. Correia (Editor), *COST 259 - Wireless flexible Personalized communications*, Final Report, John Wiley & Sons, May 2001.
- [9] L.J. Greenstein, V. Erceg, Y.S. Yeh, and M.V. Clark, A new path-gain/delay-spread propagation model for digital cellular channels, *IEEE Trans. on Veh. Technol.*, vol. 46, no. 2, pp.477-485, May 1997.